P450 Active Site Architecture and Reversibility: Inactivation of Cytochromes P450 2B4 and 2B4 T302A by *tert*-Butyl Acetylenes†

Anna L. Blobaum,‡ Danni L. Harris,§ and Paul F. Hollenberg*,‡

Department of Pharmacology, The University of Michigan, Ann Arbor, Michigan 48109, and Molecular Research Institute, Mountain View, California 94043

Received September 28, 2004; Revised Manuscript Received December 10, 2004

ABSTRACT: The inactivations of P450 2B4 and the T302A mutant of 2B4 by *tert*-butyl acetylene (tBA) and the inactivation of 2B4 T302A by *tert*-butyl 1-methyl-2-propynyl ether (tBMP) have been investigated. tBA and tBMP inactivated both enzymes in a mechanism-based manner with the losses in enzymatic activity corresponding closely to losses in P450 heme. HPLC and ESI-LC-MS analysis detected two different tBA- or tBMP-modified heme products with masses of 661 and 705 Da, respectively. Interestingly, the inactivations of the P450s 2B4 by tBA and tBMP were partially reversible by dialysis, and the tBA- or tBMP-modified heme products could only be observed with ESI-LC-MS/MS when the inactivated samples were acidified prior to analysis, indicating a requirement for protons in the formation of stable heme adducts in both the wild-type and mutant 2B4 enzymes. Results of studies using artificial oxidants to support enzyme inactivation suggest that the oxenoid-iron activated oxygen species is preferentially utilized during the inactivation of the P450s 2B4 by tBA. These results argue against the use of a peroxo-iron species by P450 2B4 T302A. Molecular dynamics studies of wild-type P450 2B4 reveal that contiguous hydrogen bond networks, including structural waters, link a conserved glutamate (E301) to the distal oxygen of the peroxo-heme species via threonine 302. Interestingly, models of 2B4 T302A reveal that a compensatory, ordered hydrogen bond network forms despite the removal of T302. These results indicate that while T302 may play a role in proton delivery in the formation of the oxenoid−iron complex and in the stabilization of acetylene heme adducts in 2B4, it is not essential for proton delivery given the presence of E301 in the binding site.

The cytochromes P450[1] constitute a superfamily of heme-thiolate enzymes involved in the metabolism of numerous endogenous and exogenous substrates (*1*, *2*). The P450 catalytic cycle involves a rich set of redox and acid−base chemistries wherein a sequential two-electron reduction of molecular oxygen induces proton additions to generate reactive oxygen intermediate(s) and water (*3*). Although generally considered to be a detoxification process, these reactions can also produce metabolic products that have a higher toxicity and/or carcinogenicity than the parent compound (*4*, *5*). In the case of mechanism-based inactivators, catalysis produces a highly reactive intermediate capable of inactivating the P450 through three distinct mechanisms: (1) *N*-alkylation of the heme moiety, (2) covalent modification of the apoprotein, and (3) cross-linking of the heme to the apoprotein (*6*).

Information about the active site architecture of P450 enzymes and the critical amino acid residues in the active site that are involved in substrate binding and catalysis has come primarily from site-directed mutagenesis studies (*7*, *8*) and from the crystal structures of bacterial and mammalian P450s (*9*−*15*). Such studies have revealed that polar and/or acidic amino acids in conjunction with ordered waters play a vital role in both stabilizing oxy intermediates in the P450 enzymatic cycle and determining the efficacy and nature of the proton transport crucial to the formation of the active species responsible for monoxygenase activity.

Mechanism-based inactivators that bind covalently to amino acid side chains have been used to identify peptides or amino acid residues in the active site that are involved in the metabolism of substrate. Studies with the P450 2B rat and rabbit enzymes using the acetylenic inactivators 2-ethynylnaphthalene (2EN) and 9-ethynylphenanthrene have been successful in identifying such critical residues (*16*−*19*). 2-Ethynylnaphthalene was found to inactivate P450s 2B1 and 2B4 in a mechanism-based manner through covalent modification of the apoproteins by a reactive ketene intermediate that bound to the threonine 302-containing I helix of the enzymes. Further studies with a P450 2B4 T302A mutant demonstrated that the rate of inactivation and covalent binding were greatly decreased in this enzyme, although the

† This publication was supported by National Institutes of Health Grants CA 16954 (P.F.H.), GM 07767 (A.L.B.), DA 017029 (A.L.B.), and R43-DC-6925 (D.L.H.).

* To whom correspondence should be addressed. Phone: (734) 764-8166. Fax: (734) 763-5387. E-mail: phollen@umich.edu.

‡ The University of Michigan.

§ Molecular Research Institute.

[1] Abbreviations: P450, cytochrome P450; tBA, *tert*-butyl acetylene; tBMP, *tert*-butyl 1-methyl-2-propynyl ether; reductase, NADPH−cytochrome P450 reductase; DLPC, dilauroyl-L-α-phosphatidylcholine; 7-EFC, 7-ethoxy-4-(trifluoromethyl)coumarin; 7-HFC, 7-hydroxy-4-(trifluoromethyl)coumarin; BSA, bovine serum albumin; TFA, trifluoroacetic acid; HPLC, high-performance liquid chromatography; ESI-LC-MS, electrospray ionization liquid chromatography−mass spectrometry; ESI-LC-MS/MS, electrospray ionization liquid chromatography−mass spectrometry/mass spectrometry.

10.1021/bi0478953 CCC: $30.25
Published on Web 02/15/2005

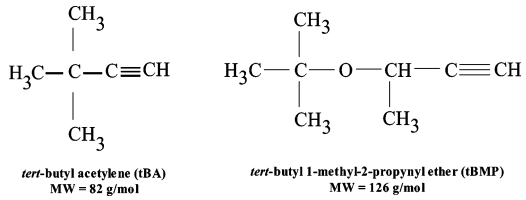

FIGURE 1: Structures of *tert*-butyl acetylene (tBA) and *tert*-butyl 1-methyl-2-propynyl ether (tBMP).

mutant was functionally able to metabolize 2EN to its ketene product (*20*). These results suggest the involvement of this highly conserved threonine residue in the P450 inactivation event. Additionally, acetylenic mechanism-based inactivators that label the heme moiety have been used to investigate more mechanistic aspects of P450 metabolic reactions including substrate positioning and orientation over the heme plane and the accessibility of the heme pyrrole rings to adduction by reactive intermediates (*21*−*25*).

Increasing experimental evidence suggests that the highly conserved threonine residue in P450 2B4 (T303 in P450 2E1, T302 in P450 2B4, and T252 in $P450_{cam}$) may be involved in a proton delivery network to the P450 active site (*26*−*30*). In P450 catalysis, reduction of molecular oxygen involves a progressive transition from a peroxo-iron activated oxygen species to a hydroperoxo-iron and finally to an oxenoid−iron complex. In addition to the generally accepted oxenoid−iron complex, Vaz and co-workers have demonstrated that the peroxo- and hydroperoxo-iron species are also competent oxidants and, depending on the particular substrate or P450 isozyme involved, any of the three species may serve as the primary oxidant in P450-catalyzed reactions (*31*). For instance, when comparing P450s 2B4 and 2B4 T302A, Vaz et al. demonstrated that there was a disruption in proton transfer leading to the oxenoid-iron species in the T302 mutant of the enzyme which resulted in a loss in the hydroxylation reactions in this enzyme and the preferential formation and utilization of a peroxo-iron intermediate in P450 substrate oxygenation (*29*). In contrast, the wild-type 2B4 enzyme preferentially utilized the oxenoid-iron species, suggesting a role for the conserved threonine in proton delivery to the 2B4 active site.

Recently, we have described the mechanism-based inactivation of P450s 2E1 and 2E1 T303A by the small acetylene, tBA (*32*). The structure of this acetylenic inactivator is shown in Figure 1. Interestingly, in contrast to the tBA-inactivated wild-type enzyme, the losses in the activity, the P450 reduced CO spectrum, and the native P450 heme of the tBA-inactivated T303A mutant were reversible with dialysis (*32*, *33*). The irreversible formation of covalent heme adducts observed with the tBA-inactivated wild-type enzyme could be mimicked with the T303A mutant if the inactivated samples were acidified with 0.1% TFA, suggesting that an exogenous source of protons was necessary for the formation of stable heme adducts in the mutant enzyme (*33*). Together, these data suggested an important role for the highly conserved threonine 303 as a participant in a proton relay network to the active site of P450 2E1.

In addition, we have previously characterized a larger acetylene, tBMP (Figure 1), as a mechanism-based inactivator of P450 2B4 (*34*) and P450s 2E1 and 2E1 T303A (*32*). When the kinetics of inactivation of these enzymes by tBMP were compared, the larger acetylenic compound proved to be a far better inactivator of P450 2B4 than the P450s 2E1 in terms of the K_I, k_{inact}, and $t_{1/2}$ values. The inactivations of the P450s 2E1 by tBMP were primarily due to covalent modification of the P450 heme by tBMP-reactive intermediates. ESI-LC-MS and MS/MS analysis of the tBMP adducts showed that both had masses of 705 Da, consistent with the mass of an iron-depleted heme plus the masses of a tBMP molecule and one oxygen atom. Most importantly, the inactivations of the P450s 2E1 by tBMP were completely irreversible by extensive dialysis (*32*). Similar to the tBMP-inactivated P450s 2E1, losses in the P450 reduced CO spectrum of tBMP-inactivated P450 2B4 corresponded to losses in native heme and the concomitant appearance of two tBMP heme adducts with *m*/*z* values of 705 Da. However, P450 2B4 samples inactivated by tBMP displayed a greater loss in enzymatic activity than could be accounted for by the reduced CO spectral or heme loss (*34*). These observations suggest that the inactivation of the wild-type P450 2B4 by tBMP is mediated through a combination of heme and protein modification, although a protein adduct was not detected through LC-MS analysis. In contrast to the P450s 2E1, inactivation of P450 2B4 by tBMP was partially reversible with overnight dialysis (*34*).

The use of mechanism-based inactivators that modify the heme prosthetic moiety of P450s where critical mutations of residues in the O_2 binding cleft have been made can provide a sensitive probe of local structure and dynamics of polar/acidic residues and associated waters crucial to the formation and transformation of the P450 activated oxygen species. In the absence of detailed cryogenic crystallographic structural information of mammalian P450s in their active intermediate and precursor states, inferences from such mutational studies provide essential data to glean structural information regarding transient intermediates and mechanism in mammalian P450s. In an attempt to further elucidate the role of the conserved threonine 302 residue in P450-catalyzed reactions and the influence of small changes in inactivator structure on metabolism by P450s, we have investigated and compared the inactivation of P450 2B4 and its T302A mutant by tBA and the larger tBMP. In contrast to what has previously been reported with the aligned T303 residue in P450 2E1 (*33*), our data on the reversible inactivation of P450s 2B4 and 2B4 T302A by tBA and tBMP indicate that the conserved T302 residue is not involved in the delivery of protons required to form stable acetylene heme products nor is the residue critical for the observed reversibility. In contrast to P450 2E1, the P450 2B4 active site is shown to be considerably larger with critical residues located at distances further away from the heme moiety allowing for the observed reversibility with tBA and tBMP in both the wild-type and T302A mutant P450s. Critical residues, such as a conserved glutamate 301, in the P450s 2B4 contribute to a hydrogen bond network in the enzyme active sites that may be operational even without the conserved T302 residue in the mutant enzyme.

EXPERIMENTAL PROCEDURES

Materials. tBA and tBMP were purchased from Aldrich Chemical Co. (Milwaukee, WI). Dilauroyl-L-α-phosphatidylcholine (DLPC), NADPH, catalase, Sephadex G-50 matrix, and BSA were purchased from Sigma Chemical Co.

(St. Louis, MO). 7-Ethoxy-4-(trifluoromethyl)coumarin (7-EFC) was obtained from Molecular Probes, Inc. (Eugene, OR). HPLC-grade acetonitrile was from Fisher (Pittsburgh, PA), and trifluoroacetic acid (TFA) was from Pierce (Rockford, IL).

Enzymes. The cDNAs for rabbit P450s 2B4 and 2B4 T302A (generously provided by L. Waskell, Veteran Affairs Health Service, Ann Arbor, MI, and M. J. Coon, The University of Michigan, Ann Arbor, MI, respectively) were expressed in *Escherichia coli* cells. Expression and purification of the proteins were carried out according to published methods (*35*, *36*). NADPH−P450 reductase was purified after expression in *E. coli* Topp3 cells as previously described by Hanna et al. (*36*).

Enzyme Activity Assays. Purified rabbit cytochrome P450s 2B4 and 2B4 T302A were reconstituted with reductase and lipid for 45 min at 4 °C. Primary incubation mixtures contained 1 nmol of P450, 2 nmol of reductase, 166 μg of DLPC, 2000 units of catalase, tBA, or tBMP (in 1 μL of CH_3OH/mL), and 1.2 mM NADPH in 50 mM potassium phosphate buffer (pH 7.4) for a total reaction volume of 1 mL. Methanol was added to the control samples instead of tBA or tBMP. At the indicated times, 25 μL of the P450 primary reaction mixture was transferred into 975 μL of a secondary reaction mixture containing 100 μM 7-EFC, 0.2 mM NADPH, and 40 μg of BSA/mL in 50 mM potassium phosphate buffer (pH 7.4). Samples were incubated for 10 min at 30 °C in a shaking water bath, and enzyme activity was terminated by the addition of 334 μL of acetonitrile. Activity was assessed spectrofluorometrically by measuring the extent of *O*-deethylation of 7-EFC to 7-HFC on an SLM-Aminco Model SPF-500C spectrofluorometer with excitation at 410 nm and emission at 510 nm (*37*).

Spectrophotometric Quantitation. P450s 2B4 and 2B4 T302A were reconstituted and inactivated as described above for enzymatic activity. One hundred microliter aliquots of control and tBA-inactivated P450 2B4 and 2B4 T302A or tBMP-inactivated 2B4 T302A primary reaction mixtures were removed and diluted with 900 μL of ice-cold 50 mM potassium phosphate buffer (pH 7.7), containing 40% glycerol and 0.6% Tergitol NP-40. The samples were gently bubbled with carbon monoxide for approximately 90 s, and the spectrum was recorded from 400 to 500 nm on a DW2 UV/vis spectrophotometer (SLM Aminco, Urbana, IL) equipped with an OLIS spectroscopy operating system (On-Line Instrument Systems, Inc., Bogart, GA). Dithionite was added, and the P450 reduced CO spectrum was recorded (*38*). The maximal absorbance at 450 nm was used to quantitate P450 heme.

HPLC Analysis. P450s 2B4 and 2B4 T302A were reconstituted and inactivated as described above for enzymatic activity. P450s 2B4 and 2B4 T302A and reductase from control and tBA- or tBMP-inactivated samples were separated by HPLC on a 250 × 4.60 mm Phenomenex reverse-phase C4 column (solvent A, 0.1% TFA and H_2O; solvent B, 95% acetonitrile and 0.1% TFA). The flow rate was 1 mL/min, and a linear gradient of 40% B to 100% B over 45 min was used. The elution of proteins and heme was monitored using diode array detection.

Irreversibility of Inactivation. P450s 2B4 and 2B4 T302A were reconstituted as described above for enzymatic activity. Control samples and samples containing tBA-inactivated P450 2B4 and 2B4 T302A or tBMP-inactivated 2B4 T302A (0.5 mL) were dialyzed overnight at 4 °C against 2 × 500 mL of 50 mM potassium phosphate buffer (pH 7.4), containing 20% glycerol, to determine whether the inactivation, P450 reduced CO spectral losses, and losses in native heme were reversible. After dialysis, samples were reconstituted with lipid and in some cases fresh reductase. Samples were assayed concurrently for 7-EFC *O*-deethylation activity, reduced CO spectrum, and heme content both prior to and after overnight dialysis.

ESI-LC-MS/MS. P450s 2B4 and 2B4 T302A were reconstituted and inactivated as described above for enzymatic activity. Primary incubation mixtures contained 0.4 nmol of P450 2B4 or P450 2B4 T302A, 0.8 nmol of reductase, and 30 μg of DLPC. Both non- and preacidified (0.1% TFA) control samples incubated with tBA or tBMP in the absence of NADPH as well as tBA-inactivated P450 2B4 and 2B4 T302A or tBMP-inactivated 2B4 T302A samples were resolved on a 150 × 2.00 mm Phenomenex reverse-phase C4 column under nonacidic solvent conditions (solvent A, H_2O; solvent B, acetonitrile) equilibrated with 40% B at a flow rate of 0.3 mL/min. Heme components were eluted using a linear gradient to 100% B over 25 min. MS/MS analysis of the tBA- or tBMP-modified heme products (*m*/*z* of 661 or 705 Da) was performed on a Thermoquest LCQ ion trap mass spectrometer with 1.0 *m*/*z* isolation width and 35% collision energy.

Alternate Oxidant-Supported Activity and Inactivation. Assay conditions were optimized to support 7-EFC enzymatic activity prior to proceeding with the inactivation studies. P450s 2B4 and 2B4 T302A were incubated with lipid for 45 min at 4 °C. Primary incubation mixtures contained 1 nmol of P450, 166 μg of DLPC, tBA (in 1 μL of CH_3OH/mL), and 1 mM hydrogen peroxide or 10 μM cumene hydroperoxide in 50 mM potassium phosphate buffer (pH 7.4) for a total reaction volume of 1 mL. Methanol or the appropriate alternate oxidant was added to the control samples instead of tBA. At the indicated times, 25 μL of the P450 primary reaction mixture was transferred into 975 μL of a secondary reaction mixture containing 100 μM 7-EFC, 40 μg of BSA/mL, and 1 mM hydrogen peroxide or 10 μM cumene hydroperoxide in 50 mM potassium phosphate buffer (pH 7.4). Samples were incubated for 10 min at 30 °C in a shaking water bath, and enzyme activity was terminated by the addition of 334 μL of acetonitrile. Activity was assessed spectrofluorometrically by measuring the extent of *O*-deethylation of 7-EFC to 7-HFC as described previously in Experimental Procedures. HPLC and diode array analysis were used to detect the formation of tBA adducts to the hemes of P450s 2B4 and 2B4 T302A in the alternate oxidant-supported system.

Construction and Assessment of Models of P450 2B4 and P450 2B4 T302A. Models of the P450s 2B4 in the peroxo- and oxyferryl heme states were prepared on the basis of the recent crystal structure of inhibitor-bound P450 2B4 as well as recent models of P450 2B4 based on the 2C isozymes. Models of the peroxo and oxyferryl heme P450s were prepared in the XLEAP module of AMBER employing both the coordinates of the crystal structure (*13*) and model P450 2B4 coordinates (*39*). Standard AMBER6 parametrization was employed (*40*) in addition to peroxo- and oxyferryl heme parametrization based on unrestricted nonlocal density

functional theoretical calculations employing a B3LYP functional and an Fe(LACVP**)/N,O,S,C(6-31G**) basis set description (*41*). The heme intermediate atomic charges were fitted to the computed molecular electrostatic potential surface of a full protoporphyrin IX model using a restrained RESP fitting procedure at the fully optimized geometries.

Models of P450 2B4 (*39*) have been reported that contain detailed descriptions of the methods of construction and critical model assessment including energetic and geometric criteria. Critical model assessments involving comparison with high-quality crystal structures to detect steric/geometrical violations as well as examination of the quality of the predicted fold commensurate with sequence via Prosa scoring were performed (*42*). In addition, stringent tests were applied in that the models were used to predict quantitative binding affinities (*39*) and metabolism (*41*, *43*) of marker substrates.

Briefly described, models of 2B4 in the present work were constructed by pairwise sequence alignments with 2C isozymes, backbone coordinate transfer between template and target in structurally conserved regions, annealing with energetic and topological constraints were used in regions apart from the structurally conserved regions using both Sali's Modeler (*44*) and thermal annealing through constrained molecular dynamics using AMBER (*40*). Following backbone construction, SCWRL rotamer libraries (*45*, *46*) were used to construct initial side chain orientations for residues not conserved between target and template sequences, and side chain (coordinate) copying was used for those side chains of residues conserved between target and template. An exception was made in the region of the residues of the I and J helix known to be associated with residues around the O_2 binding cleft. Despite the presence of a high conservation of residues in the 2C enzymes, some structural variability exists in the 2C5 structures in the positioning of the E277 residue. Given the plasticity in this region apparent in the 2C5 structures, rotamer libraries were used to "predict" the lowest energy configurations of amino acids in the 2B4 O_2 binding cleft. Unlike models of 2E1 developed in an equivalent manner, multiple rotameric states of 2B4 E301 were found to be possible with the lowest energy configurations of E301 exposed in the substrate binding site cavity. The initial model of 2B4 was then energy-structure minimized, and structural water positions were added via a previously reported procedure (*47*). The model is then energy minimized for 4000 steps, followed by equilibration for 600−1000 ps with harmonic constraints gradually removed in the process. As described previously, the largest structural shifts, side chain reorientations, and hydrogen bond pattern generation occur in the first 200 ps of such equilibration, with energetic changes substantially diminished by 600 ps (*41*). The model is then re-energy minimized for 4000 steps and subjected to a battery of geometric [Prostat and Procheck (*48*)] and energetic [ProsaII (*42*)] assessments verifying its quality compared to high-quality crystal structures as well as establishing the adequacy of its native fold consistent with sequence.

Ligand Construction and Parametrization. tBA and tBMP were initially constructed in MOLDEN. The ligand charges were derived from B3LYP DFT computations by RESP (*49*) charge fitting to the ligand molecular electrostatic potential surfaces at the DFT optimized geometries. The DFT optimized geometries were imported into the XLEAP module of AMBER6 (*50*). AMBER6 van der Waals parameters were employed for both substrates in AMBER energy minimization and dynamics studies.

Autodock Energy-Based Docking. Autodock3 (*51*) was used to identify alternative binding configurations of tBA and tBMP in the models of P450 2B4 and 2B4 T302A using an oxyferryl and peroxo representation of the heme based on both the 2B4 crystal structure and previous homology models. Low-energy docked configurations were sought, employing the Larmarkian Genetic algorithm in Autodock given its robust results independent of the initial ligand configuration. Multiple low-energy configurations were detected over a 5−10 kcal/mol window using this approach. Docking was performed using a (120 × 120 × 120) point grid and at two different grid-map spacings: (1) 0.375 Å and (2) 0.1 Å spacing. In general, the results were consistent for docked configurations in the heme/substrate binding region. The lowest energy docked configurations from the fine grid docking were then extracted for distance/configuration analysis and as initial ligand/CYP2B4 configurations for subsequent MD simulations using AMBER6 in an all-hydrogen representation to examine the dynamic stability of such configurations relative to the binding site amino acids.

AMBER Molecular Dynamics. Molecular dynamics simulations were performed on the basis of initial Autodock3 low-energy docked configurations with the heme in either the oxyferryl or peroxo forms. The purpose of performing the dynamics studies was to verify the dynamic temporal stability of such docked complexes including bound inactivator, modeled protein, and structural waters and to examine the time-dependent interactions of the substrate relative the oxyferryl center. In addition, we compared the nature of the hydrogen bond networks present in the enzyme active site, including a network thought to involve the O_2 binding cleft conserved threonine, bound waters, and a nearby conserved acidic glutamate residue thought to possibly play a role in the proton transport chain involved in formation of the oxyferryl heme species from the reduced dioxygen heme species.

Initial MD equilibrations of the wild-type 2B4 and 2B4 T302A bound ligand configurations were conducted using a 12 Å potential truncation, a radial screened ($D = r$) dielectric model, and a 1 fs integration time step employing NVT dynamics. Four hundred picosecond dynamics simulations of P450-substrate dynamics were conducted at 300 K and included all protein and modeled structural waters in addition to the inactivators. After gleaning initial behavior from these approximate radial-dielectric simulations, simulations were conducted employing full protein solvation in a box of water of initial dimensions 80 Å × 68 Å × 74 Å at constant pressure and 300 K. Following 200 ps of equilibration, short production dynamics runs of 200 ps length were performed. All simulations were executed using the SANDER module of AMBER6 on the Cray T3E at the Pittsburgh Supercomputer Center.

RESULTS

Inactivation of P450s 2B4 and 2B4 T302A. The kinetics for the inactivation of P450 2B4 and the T302A mutant of 2B4 by tBA were studied by measuring the loss in 7-EFC

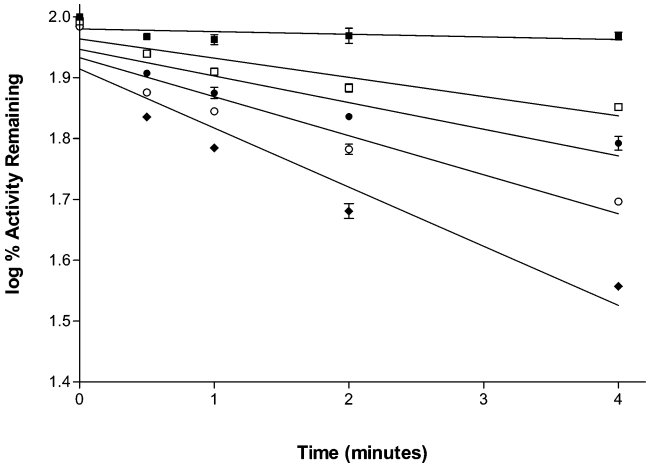

FIGURE 2: Time- and concentration-dependent loss of P450 2B4 7-EFC O-deethylation activity following incubation with tBA and NADPH. At the indicated time points, samples were removed from the primary reaction mixture and assayed for 7-EFC activity. The concentrations of tBA were (■) 0, (□) 33, (●) 67, (○) 167, and (◆) 333 μM. The data shown represent the mean and standard deviation from three to five separate experiments. For some data points, the deviation was smaller than the size of the symbol.

Table 1: Kinetic Constants for the Inactivation of P450s 2B4 by tBA[a]

sample	K_I (μM)	k_{inact} (min^{-1})	$t_{1/2}$ (min)
P450 2B4	75	0.23	3.0
P450 2B4 T302A	20	0.09	8.0

[a] Assay conditions were as described in Experimental Procedures.

O-deethylation activity. P450 2B4 in the reconstituted system was inactivated by tBA in a time- and concentration-dependent manner (Figure 2). In the absence of NADPH, there was no significant loss in the activity of the enzyme with tBA (data not shown). As can be observed in Figure 2, the inactivation followed pseudo-first order kinetics. The apparent kinetic constants were determined from a double reciprocal plot of the inverse of the initial rates of inactivation as a function of the reciprocal of the tBA concentration (data not shown) and are summarized in Table 1. The maximal rate of inactivation (k_{inact}) of P450 2B4 by tBA was 0.23 min^{-1}, the concentration of tBA required for half-maximal inactivation (K_I) was approximately 75 μM, and the half-time for inactivation ($t_{1/2}$) was 3 min. The T302A mutant of 2B4 was also inactivated by tBA in a time-, concentration-, and NADPH-dependent manner (data not shown). For comparison, the apparent kinetic constants for the inactivation of P450 2B4 T302A by tBA are shown in Table 1. The concentration of tBA required for half-maximal inactivation of the T302A mutant was similar to that of the wild-type enzyme (approximately 20 μM). Likewise, the maximal rate of inactivation of the T302A mutant by tBA (0.09 min^{-1}) and the half-time for inactivation (8 min) were comparable to the inactivation of the wild-type enzyme. Moreover, if the efficiency of the inactivator is calculated by dividing the k_{inact} by the K_I, similar values are obtained, indicating that there is no significant difference in the efficiency of the inactivations of the two 2B4 P450s by tBA.

Previous studies in our laboratory have characterized tBMP as a mechanism-based inactivator of P450 2B4 (*34*). To examine the role of the conserved threonine 302 residue in the inactivation event, we have also determined the kinetics of inactivation of P450 2B4 T302A by tBMP. The concentration of tBMP required for half-maximal inactivation (K_I) was approximately 3 μM, and the half-time for inactivation ($t_{1/2}$) was 3 min (data not shown). These apparent kinetic constants are similar for what has been previously described for tBMP inactivation of the wild-type P450 2B4 (*34*).

Table 2: Partial Restoration in the Activity, P450 Reduced CO Spectrum, and Native Heme of tBA-Inactivated P450s 2B4 Following Dialysis[a]

	% activity remaining	% P450 reduced CO spectrum remaining	% heme remaining		
			A	B	C
P450 2B4 (before dialysis)	30 ± 4	51 ± 9	34	5	23
P450 2B4 (after dialysis)	55 ± 7	76 ± 7	62	ND	2
P450 2B4 T302A (before dialysis)	52 ± 4	93 ± 5	42	10	10
P450 2B4 T302A (after dialysis)	74 ± 2	81 ± 10	73	ND	2

[a] Assay conditions were as described in Experimental Procedures. Enzymatic activity, reduced CO complex formation, and P450 heme were measured before and after dialysis. The value obtained for the noninactivated sample in each condition was assigned 100% and the numbers shown were calculated as percent of control activity, P450 reduced CO spectrum, and P450 heme remaining, respectively. The data shown represent the mean and standard deviation from three to five separate experiments, except for the heme studies in which the data shown are an average of values obtained from two independent experiments each done in duplicate. Spectrophotometric quantitation was used to determine the reduced CO spectrum.

Spectrophotometric Quantitation. The effect of tBA inactivation on the P450 reduced CO complex formation of P450s 2B4 and 2B4 T302A was examined. The data in Table 2 show that the inactivation of wild-type P450 2B4 by tBA resulted in significant losses in enzymatic activity (30 ± 4% activity remaining) that were accompanied by simultaneous decreases in the P450 CO spectrum (51 ± 9% reduced CO spectrum remaining). When the T302A mutant of 2B4 was inactivated by tBA, 52 ± 4% of the enzymatic activity remained following inactivation. However, in contrast to the wild-type enzyme, the tBA-inactivated T302A mutant was still able to form a P450 reduced CO complex (93 ± 5% remaining). As the tBA-inactivated T302A mutant demonstrates time-, concentration-, and NADPH-dependent loss in enzymatic activity, the ability of this sample to form a reduced CO complex suggested that the inactivator was bound primarily either to the apoprotein or to the P450 heme in such a way that CO was still able to bind.

HPLC Analysis of P450s 2B4 and 2B4 T302A. P450s 2B4 and 2B4 T302A were inactivated by tBA and analyzed to determine the amount of native heme remaining after inactivation and to determine whether heme-acetylene adducts could be detected. The amount of heme remaining in the tBA-inactivated P450 2B4 and 2B4 T302A samples was measured using HPLC with diode array detection. Table 2 shows that for the inactivation of P450 2B4 by tBA, the percentage loss in enzymatic activity correlated with the percentage decrease in the P450 reduced CO complex and the loss in native heme detected using HPLC. Interestingly, inactivation of the T302A mutant by tBA resulted in a significant loss in enzymatic activity (52 ± 4% remaining)

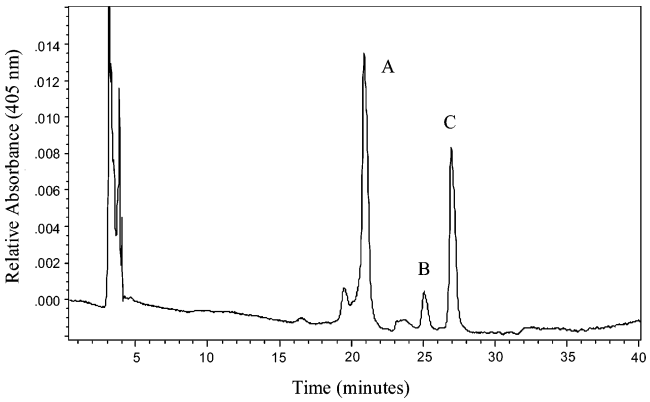

FIGURE 3: HPLC heme analysis of P450 2B4 inactivated by tBA in the presence of NADPH. The unmodified heme peak (A) elutes at 21 min, and the two heme adducts (B and C) elute at approximately 25 and 27 min, respectively.

that was not accompanied by a loss in the P450 reduced CO spectrum (93 ± 5% remaining). Although the tBA-inactivated T302A mutant sample was still able to form a reduced CO complex, losses in the enzymatic activity and in the native P450 heme were comparable. These observations suggest that the metabolism of tBA by P450s 2B4 and 2B4 T302A leads to the formation of tBA reactive intermediates that modify the P450 heme and subsequently inactivate these enzymes. Figure 3 shows the HPLC profile at 405 nm of P450 2B4 incubated with tBA and NADPH. In addition to the native heme eluting at approximately 21 min (A), two additional peaks (B and C) were observed eluting at approximately 25 and 27 min, respectively. The tBA-inactivated 2B4 enzyme exhibited about 5 times more of peak C than peak B. Only peak A, corresponding to the unmodified heme, was observed in control incubations where the P450 was incubated with tBA in the absence of NADPH (data not shown). The diode array spectra of the native heme and the tBA-modified hemes (peaks B and C) were similar with the exception of a small shift toward longer wavelengths for the modified hemes, consistent with the formation of *N*-alkylated heme products (data not shown). Inactivation of the 2B4 T302A mutant by tBA also resulted in the formation of two tBA adducts to the P450 heme with retention times similar to those of the adducts generated with the tBA-inactivated wild-type enzyme (data not shown). Interestingly, the ratio of the two tBA adducts was 1:1 in the T302A samples, suggesting an alteration in the structure of the active site of the mutant enzyme that changed the specificity of heme adduct formation.

Previous studies from our laboratory have reported on the mechanism for the inactivation of P450 2B4 by tBMP (*34*). Inactivation of the wild-type enzyme by tBMP resulted in an approximate 81 ± 4% loss in enzymatic activity, which was accompanied by a 32 ± 5% loss in the P450 reduced CO spectrum and a 49 ± 10% loss in native heme. Although a protein adduct was not detected with LC-MS analysis, the difference between the loss in catalytic activity and the loss in native heme suggested that the inactivation of wild-type 2B4 by tBMP may be due to modification of both the heme and apoprotein. To investigate the role of the conserved threonine 302 residue in the inactivation event, we characterized the mechanism for the inactivation of the T302A mutant of P450 2B4 by tBMP. Losses in enzymatic activity (50 ± 3%) corresponded to losses in native heme (58 ± 6%), suggesting that tBMP modification of the P450 heme was the primary mechanism leading to inactivation of the T302A mutant. The HPLC profile at 405 nm of P450 2B4 T302A incubated with tBMP and NADPH showed the elution of native heme at approximately 21 min (A) and two additional peaks (B and C) at approximately 26 and 28 min, respectively (data not shown). In comparison to the tBA-inactivated T302A enzyme, the later elution times observed for the B and C adducts presumably correspond to the larger tBMP molecule being adducted to the P450 heme. The tBMP-inactivated 2B4 T302A enzyme generated about 5 times more of peak B than peak C. Only peak A, corresponding to the unmodified heme, was observed in control incubations where the P450 was incubated with tBMP in the absence of NADPH (data not shown). The diode array spectra of peaks B and C from the tBMP-inactivated samples were similar to the spectrum of the native heme, supporting the suggestion that both peaks are tBMP-modified heme products.

Irreversibility of the Inactivation of P450 2B4 and 2B4 T302A. The inactivation of P450 2E1 T303A by tBA was previously shown to be completely reversible (restoration of activity and the reduced CO spectrum to 100%) with an overnight dialysis (*32*). Control and tBA-inactivated P450 2B4 and 2B4 T302A samples were dialyzed extensively to determine whether the inactivation by tBA was reversible (Table 2). Additionally, the samples were tested before and after dialysis to determine whether losses in native heme and the P450 reduced CO spectrum could be reversed. Interestingly, both the inactivation and the losses in native heme of the tBA-inactivated P450s were partially reversible. Approximately 20% of the P450 2B4 and 2B4 T302A activity and 30% of the native heme could be recovered following an overnight dialysis (Table 2). In addition, dialysis caused a significant decrease in both of the tBA heme adducts for the tBA-inactivated P450 2B4 and T302A samples. In the tBA-inactivated wild-type samples, a restoration of approximately 20% of the reduced CO spectrum was also observed. No significant change in the reduced CO spectrum was observed for the tBA-inactivated T302A mutant. Addition of fresh reductase to the dialyzed samples did not affect the loss in activity (data not shown), indicating that the inactivation is due to modification of the P450 enzymes and not the reductase.

Approximately 10−20% reversal in the inactivation of P450 2B4 by tBMP following overnight dialysis or spin column gel filtration has been reported (*34*). Here, we report that tBMP inactivation of the T302A mutant was also partially reversible with overnight dialysis. Losses in activity, the reduced CO spectrum, and native heme were restored by approximately 20−30% following an overnight dialysis. Dialysis also resulted in a reduction in adduct C with a concurrent recovery of native heme for the tBMP-inactivated T302A samples (data not shown). Interestingly, adduct B was stable to overnight dialysis, suggesting that the primary source for the recovery of native heme was the degradation of adduct C. The stability of B adduct to dialysis is unique in that both the B and C adducts in the tBA-inactivated P450 samples were significantly reduced following an overnight dialysis. The internal oxygen atom within the larger tBMP molecule may provide a surface for hydrogen bonding with nearby residues in the 2B4 T302A active site. It is possible

Table 3: ESI-LC-MS/MS Analysis of Adduct C from tBA-Inactivated P450s 2B4 and 2B4 T302A under Nonacidic Solvent Conditions[a]

	adduct C			
	parent ion (*m*/*z*)	MS/MS ion fragments (*m*/*z*)		
P450 2B4 T302A + tBA	N/O	N/O	N/O	N/O
P450 2B4 T302A + tBA (preacidified)	661.2	604.2	576.3	562.3
P450 2B4 + tBA	N/O	N/O	N/O	N/O
P450 2B4 + tBA (preacidified)	661.5	604.4	576.4	562.3

[a] P450s 2B4 and 2B4 T302A were reconstituted with reductase and lipid as described in Experimental Procedures. Control and tBA-inactivated P450 sample components were resolved by reverse-phase chromatography under nonacidic solvent conditions (water, acetonitrile). In some cases, 0.1% TFA was added to preacidify the sample prior to injection. MS/MS analysis of the tBA-modified heme products (*m*/*z* of 661 Da) was performed with 1.0 *m*/*z* isolation width and 35% collision energy. The values shown are representative of data obtained from three independent experiments. N/O indicates that no tBA-modified heme products or ion fragments were observed.

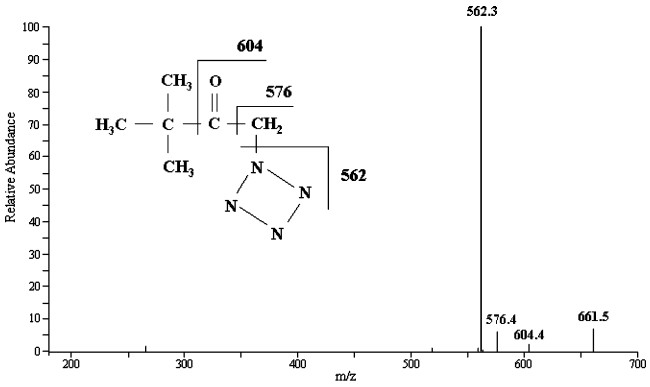

FIGURE 4: ESI-LC-MS/MS analysis of a preacidified tBA-inactivated P450 2B4 sample separated under nonacidic solvent conditions. P450 2B4 was incubated with tBA and NADPH and acidified with 0.1% TFA prior to injection onto the mass spectrometer. The main panel shows the resulting MS/MS data from the second tBA-modified heme product (adduct C), which has an overall mass-to-charge ratio of 661 Da. The inset illustrates the proposed sites of fragmentation of this adduct based on the ion fragmentation pattern observed under the MS/MS conditions.

that these interactions would lead to stabilization of adduct B in the active site, whereas adduct C would not experience these stabilizing interactions. Interestingly, the recovery of native heme in tBMP-inactivated wild-type 2B4 samples correlated only with a loss in the amount of adduct B; the second tBMP adduct was completely stable to overnight dialysis (*34*). The difference in the ratios of adduct B and C and the apparent differences in the stabilities of the adducts to dialysis with the tBMP-inactivated P450s 2B4 suggest that there has been an alteration in the active site architecture of the T302A mutant that has shifted key residues involved in stabilization of the tBMP reactive intermediate.

ESI-LC-MS/MS Analysis of Acetylene-Inactivated P450s 2B4 and 2B4 T302A under Nonacidic Solvent Conditions. Protons were previously shown to be required in the formation of stable acetylene adducts to the heme of P450 2E1 T303A but not in the wild-type P450 2E1 enzyme during inactivation by tBA (*33*). To determine whether our HPLC and ESI-LC-MS denaturing solvent conditions might be contributing to the formation and/or reversibility of the heme adducts in the tBA-inactivated 2B4 and 2B4 T302A samples, control and inactivated samples were analyzed by ESI-LC-MS/MS under nonacidic solvent conditions (water, acetonitrile) rather than the standard conditions with TFA routinely used in our studies. ESI-LC-MS/MS analysis of the tBA-inactivated P450 2B4 and 2B4 T302A samples under nonacidic solvent conditions resulted in a loss of the 661 Da masses associated with adducts B and C. Upon the addition of 0.1% TFA to the inactivated samples, the two tBA adducts with *m*/*z* values of 661 Da were observed. The data for adduct C are presented in Table 3. Similar results were observed for adduct B (data not shown). The tBA-modified heme products were only seen in acidified samples from tBA-inactivated P450s 2B4 and not in samples incubated with tBA in the absence of NADPH (data not shown). When the adduct peaks with the 661 Da masses were subjected to MS/MS analysis, the adducts fragmented into ions corresponding to a tBA molecule with an inserted oxygen atom at the internal carbon of the acetylenic group. The resultant ion fragmentation pattern for adduct C of tBA-inactivated P450 2B4 is shown in Figure 4. Table 3 shows that similar results were obtained for adduct C in tBA-inactivated T302A samples. As shown in the inset of Figure 4, the terminal carbon of the acetylenic group is attached to the heme moiety at one of the pyrrole nitrogens. The structures of adducts B and C, as determined by MS/MS analysis, are analogous to the structure reported by Dexter and Hager for the reversible adduction of allylbenzene to the heme of chloroperoxidase (*52*, *53*). However, the exact locations of the tBA adducts on the P450 heme could not be determined from our MS/MS analyses. The requirement for acidic protons to form the tBA adducts to the heme of both the wild-type and T302A mutant enzymes suggests that the T302 residue, although considered to be the functional equivalent of T303 in P450 2E1, may be not be playing the same role in proton donation to the enzyme active site or in the observed reversibility, as has previously been reported for 2E1 (*33*).

Similar to the tBA-inactivated P450s, ESI-LC-MS/MS analysis of tBMP-inactivated P450 2B4 T302A samples under nonacidic solvent conditions resulted in an absence of the 705 Da masses for adducts B and C. Upon the addition of 0.1% TFA to the inactivated samples, the two tBMP adducts with *m*/*z* values of 705 Da were observed. When the peaks exhibiting the 705 Da masses were subjected to MS/MS analysis, the two adducts displayed ion fragmentation patterns corresponding to a tBMP-adducted heme with an oxygen atom inserted at the internal carbon of the acetylenic group. The MS/MS spectral data, the ion fragmentation pattern, and the proposed structure for adduct C of tBMP-inactivated P450 2B4 T302A are shown in Figure 5 and the inset. This fragmentation pattern is similar to what has been previously reported for tBMP-inactivated P450 2B4 (*34*).

Alternate Oxidant-Supported Activity and Inactivation. A variety of artificial oxidants can replace the requirement for NADPH and molecular oxygen in P450 catalysis and have been utilized to support the formation of distinct oxidant species in the P450 catalytic cycle (*54*−*56*). As hydrogen peroxide and cumene hydroperoxide preferentially form the peroxo- and oxenoid-iron species, respectively, we examined the ability of these artificial oxidants to support the 7-EFC

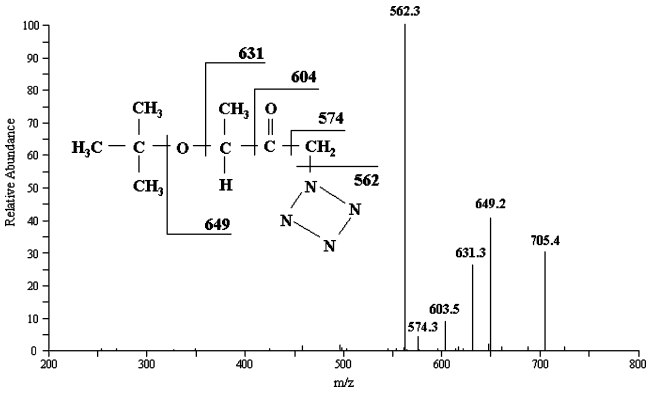

FIGURE 5: ESI-LC-MS/MS analysis of a preacidified tBMP-inactivated P450 2B4 T302A sample separated under nonacidic solvent conditions. P450 2B4 T302A was incubated with tBMP and NADPH and acidified with 0.1% TFA prior to injection onto the mass spectrometer. The main panel shows the resulting MS/MS data from the second tBMP-modified heme product (adduct C), which has an overall mass-to-charge ratio of 705 Da. The inset illustrates the proposed sites of fragmentation of this adduct based on the ion fragmentation pattern observed under the MS/MS conditions.

Table 4: Effect of the Alternate Oxidants Hydrogen Peroxide and Cumene Hydroperoxide on the Inactivation of P450s 2B4 by tBA[a]

	% activity remaining		
	HP-supported inactivation	CH-supported inactivation	type of adduct
P450 2B4	92	26	heme
P450 2B4 T302A	98	33	heme

[a] Assay conditions were as described in Experimental Procedures. P450s 2B4 and 2B4 T302A were incubated with DLPC in the absence of reductase. The alternate oxidants, hydrogen peroxide (HP) or cumene hydroperoxide (CH), were used to support the enzymatic activity of the P450s and their inactivation by tBA in a NADPH-free system. The values shown are the average from two separate experiments in which the results differed by less than 5%. The value obtained for the noninactivated sample in each condition was assigned 100%, and the numbers shown were calculated as percent of control activity remaining. The 100% control values for enzymatic activity supported by HP and CH were 0.2 and 1.0 pmol of 7-HFC min^{-1} (pmol of P450)$^{-1}$, respectively, for P450s 2B4 and 2B4 T302A. The rate of CH-supported activity was similar to the rate of NADPH-supported activity in the reconstituted system. The formation of tBA heme adducts was detected by HPLC and diode array analysis as described in Experiment Procedures.

O-deethylation activity of P450s 2B4 and 2B4 T302A as well as the inactivation of these enzymes by tBA in a reductase- and NADPH-free system. The optimal concentrations of hydrogen peroxide and cumene hydroperoxide required to support the P450 activity were found to be 1 mM and 10 μM, respectively. Therefore, these concentrations were used in subsequent experiments to determine if the two artificial oxidants could support the inactivation of the P450s 2B4 by acetylenic inactivators. Table 4 shows that hydrogen peroxide, which favors the formation of a peroxo-iron oxygen intermediate, was not able to support the inactivation of either the wild-type or T302A mutant enzymes by tBA. However, the formation of an iron-oxo intermediate through the alternate oxidant cumene hydroperoxide was able to support the inactivation of both P450s by tBA. HPLC and diode array analysis demonstrated that the mechanism of inactivation was primarily through the formation of tBA adducts to the P450 hemes (Table 4 and data not shown).

Variability of Conserved Acidic Residues Important in the Proton Transport Chain. The lack of a substantial effect of the T302A mutation on the formation of either reversible or irreversible heme adducts can be interpreted in terms of structural models of P450 2B4 in the peroxo and oxyferryl heme forms based on the mammalian crystal structures of 2B4 (*12*, *13*) and models of P450 2B4 (*39*) based on 2C isozymes (*15*, *57*). An examination of both the current crystal structures of the open/resting state (*12*) and the closed/inhibitor-bound (*13*) forms of P450 2B4, as well as models of 2B4 (*39*, *43*) developed prior to the recent report of crystal structures, has shed light on the importance of E301 and its plausible role in anchoring and stabilizing the proton transfer network essential for the formation of the oxenoid-iron-activated oxygen species.

The models of P450 2B4 have been validated by subjecting them to a battery of geometric/topological and energetic tests, as well as the prediction of substrate and inhibitor binding affinities (*39*). The latter tests bolster confidence in the utility of comparative models, developed from moderate sequence identity templates to predict substrate binding free energies and the geometric determinants of competitive metabolism from multiple sites in a substrate. Perhaps the most sensitive test of such models, however, is their scrutiny by direct comparison with the crystal structure results once they are available.

Figure 6, panel A, shows the superimposed binding site structure of the recently reported inhibitor-bound crystal structure of P450 2B4 with a model previously reported for P450 2B4 based on P450 2C9. The disposition of the residues in the binding site that form contacts with the inhibitors in this study are in reasonable agreement, while the RMS deviation in the backbone coordinates of the model and the crystal structure is 1.7 Å. Prosa normalized *z*-scores are perhaps a more evenhanded manner of assessing the quality of the model or crystal structure fold commensurate with sequence, in that the meaning of an RMSD is strongly dependent on the length of the protein (*58*). The normalized *z*-score for the 2B4 crystal structure is 0.82, while the score of the model based on the 2C9 template is 0.86. The normalized *z*-scores of the model and crystal structure are of comparable quality and the other geometric measures in the form of bond, angle, and dihedrals are found to be on par. Indeed, the distribution of docked inactivators in both the model and crystallographic based 2B4 structures is very similar and quite distinct from that of the docking distribution for 2E1 (Harris, Blobaum, and Hollenberg, in preparation).

Most germane to the theme of this work is the prediction in the model that the lowest energy configuration of E301 has exposure to the substrate/inhibitor binding site. Examination of Figure 6, panel A (structure in red), reveals the model P450 2B4 to have E301 in a conformation quite analogous to that found in the crystal structure (green).

Energy-Based Docking: Probes of Differential Active Site Architecture/Dimensions. In Figure 6, panels B and C show selected results of energy-based docking of tBA and tBMP into wild-type P450 2B4 relevant to the mechanism-based inactivation of this enzyme. No significant/interpretable differences were noted for docking into a model of T302A other than changes in the tBMP *tert*-butyl contacts with the A302. Notably in all cases, low-energy docked configurations exist with the central acetylenic carbon of the inactivator

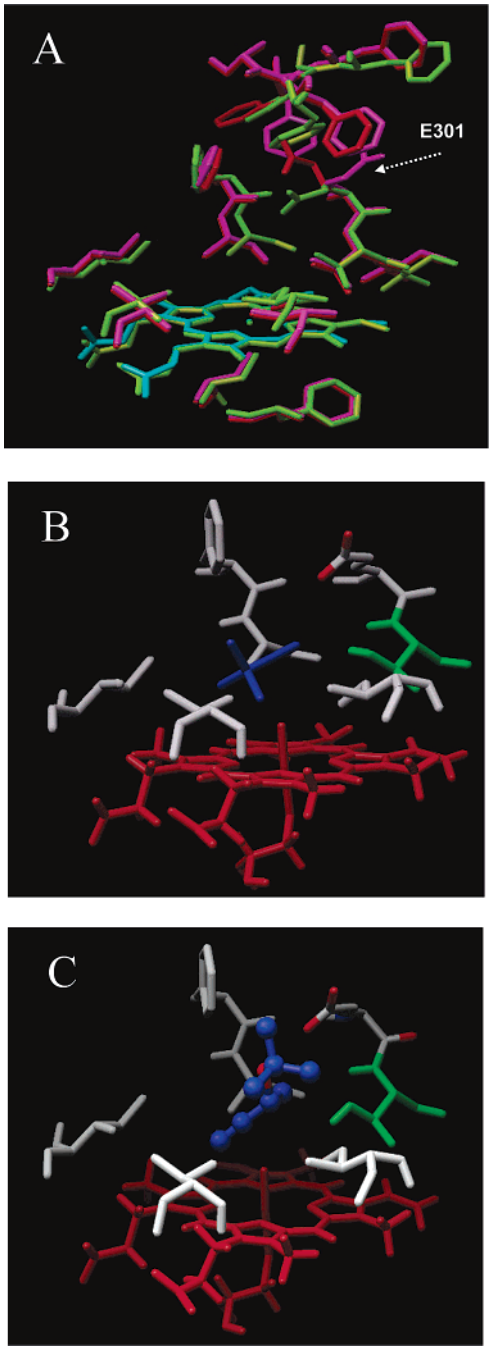

FIGURE 6: (A) Superposition of a previously reported model of P450 2B4 based on P450 2C9 (*39*) with the 4-(4-chlorophenyl)-imidazole inhibitor bound structure of P450 2B4 (*13*). Here, glutamate 301 (E301) is seen to have partial exposure in the model to the substrate/inhibitor binding site. The model has good agreement with respect to the general disposition and conformation of binding site residues contacting the acetylenic inactivators. (B, C) Docked lowest energy configurations of the acetylenic inactivators, tBA (panel B) and tBMP (panel C), in the P450 2B4 crystal structure modeled in the oxyferryl heme form. Threonine 302 (T302) is depicted in green in both panels. No significant differences in low-energy docked distributions were found in models of the 2B4 T302A mutant. Note that the central acetylenic carbons interact closely with the oxyferryl center, the configuration prerequisite for the initial oxygen addition to the unsaturated linkage.

proximate to the active oxygen species. This is precisely the configuration, indicated in ongoing density functional theoretical investigations, that is required for initiation of suicide inhibition of the heme by sequential oxygen insertion to the acetylenic center followed by addition of the terminal "acetylenic" radical center to the heme nitrogen to form an *N*-alkylated heme product. The energy-based docking results are consistent with the mass spectral results in that the mutations certainly do not significantly disfavor the binding of the inactivators proximate to the active oxygen species. While docking energy scores, as a general rule, do not give good estimates of binding free energies, the nearly equivalent docking results for the mutant and wild-type 2B4 enzymes are not in discord with the similar K_I values reported in Table 1 in this work. These results indicate that there are insignificant changes in K_I of tBA and tBMP due to mutation of the highly conserved threonine in the O_2 binding pocket. Rather, it is plausible that the mutations more directly impact the efficiency of formation of the active oxygen intermediates involved in the inactivation chemistry by modulating proton transfer steps in the activation of those oxygen intermediates crucial for metabolism.

T302A Mutational Effect on the Hydrogen Bond Networks Connecting E301 and the Peroxo Heme. Figure 7 shows snapshots extracted from dynamics of tBA bound to wild-type P450 2B4 and the T302A mutant of 2B4 based on both the recent P450 2B4 crystal structure and models of 2B4 based on P450 2C9. Figure 7, panel A, traces the hydrogen bond network connectivity involving two waters that directly "connect" the glutamate carboxylate with T302 that directly hydrogen bonds to the distal oxygen of the heme-bound peroxo species. Panel B shows a nearly identical result is recovered from simulations based on the model P450 2B4, including modeled structural waters based on 2C9 (*39*). The simulation results have significance in that such networks, when stable, facilitate proton transfer to the distal oxygen of the peroxo heme, an essential feature for activation to form the oxyferryl species. After initial construction of the model of the peroxo heme for P450 2B4 based on either the 2B4 ferric heme crystal structure or a 2C9 template, no contiguous hydrogen bond network exists. Yet, after a short equilibration, structural waters "move into place" to form a stable network connecting E301 and the peroxo heme. A temporally stable hydrogen bond network connecting acidic or polar residues to the distal oxygen is required to form the oxenoid−iron complex from the peroxo heme (*59*, *60*).

Figure 7, panel C, shows the 20 and 100 ps snapshots during a short 200 ps simulation of a model of P450 2B4 T302A based on the 2B4 crystal structure. Notably a robust hydrogen bond network forms, linking E301 and the peroxo heme despite the absence of a T302 polar side chain to orient, stabilize, and directly participate in the putative proton transfer network. While polar amino acids reduce the effective barrier for proton transfer in active oxygen formation, the presence of a charged glutamate residue anchoring a network likely facilitates the initial proton transfer events, even in the absence of a supporting role of T302.

These initial modeling studies support the conclusions drawn from the mass spectral assignments regarding the lack of a T302 mutational dependence of tBA/tBMP binding and inactivation of the heme in 2B4. The modeling results suggest the rationale behind this is twofold: (1) there is partial exposure of glutamate 301 to the P450 2B4 binding site due to the preferred E301 conformations and these conformations have some plasticity, and (2) the binding site is sufficiently large to allow entry of structural waters into positions

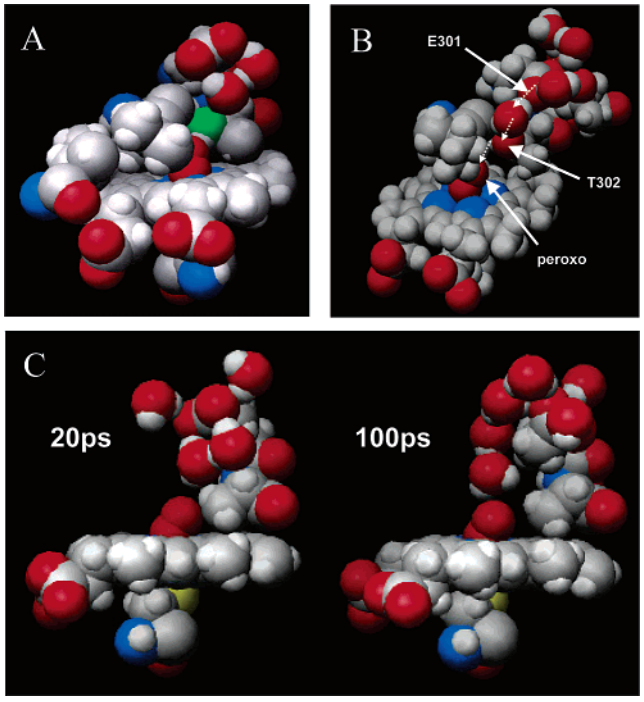

FIGURE 7: Proton delivery networks in P450s 2B4. (A) Panel A depicts a 200 ps configuration of tBA and O_2 binding cleft residues surrounding the peroxo-iron species in the tBA-bound P450 2B4 based on the 2B4 crystal structure. A contiguous hydrogen bond network exists connecting the E301 acidic side chain to the distal atom of the peroxo-iron species. In the case of wild-type P450 2B4 simulations, this connectivity occurs via T302. The oxygen of T302 is highlighted in green to emphasize its position in the network. T302 directly hydrogen bonds to the distal oxygen of the peroxo species. (B) Panel B shows that an analogous hydrogen bond network forms after 200 ps in a model of P450 2B4 based on P450 2C9 with bound (docked) tBA. Here, two hydrogen-bonded waters are shown intervening between the E301 carboxylate and the T302 hydroxyl, which then in turn hydrogen bonds directly to the distal oxygen of the peroxo heme. (C) Panel C depicts results at 20 and 100 ps in a 200 ps simulation of a model of the 2B4 T302A mutant based on the 2B4 crystal structure. Waters partially compensate for the T302A mutation by forming a network that is capable of efficient proton delivery. This relay network of protons is essential for the formation of the oxenoid-iron species, which is required for initiation of the inactivation reaction in 2B4. The tBA inhibitor has been removed from this depiction to facilitate visualization of the underlying hydrogen bond networks. The presence of the charged E301 residue and the distal oxygens of the peroxo heme serve to order the local waters, essential to completion of the proton delivery network, and appear to adequately compensate for the T302A mutation.

previously occupied by the T302 polar hydroxyl. Such water-entry-substitution motifs for T → A mutations are not uncommon in P450s and other enzymes, with the major variability in P450s being the degree to which the new network, including new water(s), stabilizes the new water occupancy (*61*, *62*). Work in progress indicates a different scenario arises in the small 2E1 binding site, illustrating the effects of mutations on such hydrogen bond networks are both P450 isoform and even substrate dependent.

DISCUSSION

Previous studies using acetylenic compounds as mechanism-based inactivators of P450s 2B4 and 2E1 and the threonine to alanine mutants of these enzymes (2B4 T302A and 2E1 T303A) have suggested the involvement of this highly conserved threonine residue in the inactivation of these P450s (*16*−*19*). Likewise, the reversible inactivation of P450 2E1 T303A by tBA has previously suggested a role for this residue in proton donation to the active site of P450 2E1 (*33*). To further investigate the role of the conserved threonine residue in P450 metabolic reactions and proton delivery, tBA was investigated as a mechanism-based inactivator of P450s 2B4 and 2B4 T302A. Since tBMP has been previously characterized as a mechanism-based inactivator of P450s 2E1 and 2E1 T303A (*32*) and of P450 2B4 (*34*), we also investigated the ability of this compound to act as an inactivator of the T302A mutant of P450 2B4.

The two acetylenes, tBA and tBMP, were found to inactivate the P450s 2B4 in a time-, concentration-, and NADPH-dependent manner with K_I values in the micromolar range (Table 1 and data not shown). The maximal rate of inactivation, k_{inact}, and the half-time for inactivation, $t_{1/2}$, were similar for tBA inactivation of P450 2B4 and the T302A mutant and for tBMP inactivation of P450 2B4 T302A. If the efficiency of the inactivator is calculated by a ratio of k_{inact}/K_I, the resultant values are comparable to one another, suggesting that tBA is an efficient inactivator of both 2B4 P450s. In related studies, 3,3-dimethyl-1-butene, the olefin analogue of tBA, was also tested for its ability to inactivate the P450s 2B4 in a mechanism-based manner (data not shown). As the olefin analogue was unable to inactivate the P450s, it appears that the acetylenic functional group of tBA is required for inactivation. When P450s 2B4 and 2B4 T302A were incubated with tBA or tBMP and NADPH, the losses in enzymatic activity correlated with losses in native heme as detected by HPLC with diode array analysis (Table 2 and data not shown). The inactivations of P450s 2B4 and 2B4 T302A by tBA and P450 2B4 T302A by tBMP were primarily due to the formation of two different tBA or tBMP heme adducts (B and C) with masses of 661 and 705 Da, respectively. The masses of the acetylene adducts (661 and 705 Da) corresponded to those expected for an iron-depleted heme, an acetylene reactive intermediate, and one oxygen atom. Interestingly, the ratios of adduct B to C differed significantly between tBA-inactivated P450 2B4 and 2B4 T302A samples (Table 3) and may reflect the relative accessibility of the different pyrrole rings in the P450 active site to the reactive intermediate. As the ratios of the two adducts also differed between tBA- and tBMP-inactivated T302A samples (data not shown), the structure of the inactivator may also influence the site of adduction and possibly the reversibility of inactivation. Current studies are underway in our laboratory to further investigate this phenomenon.

The mechanism-based inactivation of P450 2B4 by tBMP results in the formation of two tBMP adducts to the P450 heme as detected by HPLC with diode array analysis and the possible formation of a tBMP adduct to the apoprotein (*34*). LC-MS/MS and proton NMR analysis suggested that the tBMP heme adducts (B and C) result from *N*-alkylation of the A and D pyrrole rings of the P450 heme (*34*). Since the tBMP adducts of P450 2B4 T302A are similar in their retention times and MS/MS spectral patterns when compared to those formed with the wild-type enzyme, it is likely that these adducts are also on the A and D pyrrole rings. The location of these adducts on the A and D rings is in agreement with the studies of Ortiz de Montellano and co-

workers on the accessibility of these positions on the pyrrole rings for adduct formation in the reactions of P450 2E1 with phenyldiazene, (2-naphthyl)hydrazine, and *p*-biphenylhydrazine (*63*).

We have previously reported the reversible inactivation of P450 2E1 T303A by tBA (*32*). Partial reversibility was also seen with P450 2B4 that had been inactivated by tBMP (*34*). To further investigate the role of the conserved T302 residue in the 2B and 2E families of P450s and the influence of the structure of the inactivator in the reversibility, we tested whether the inactivations of P450s 2B4 by tBA and P450 2B4 T302A by tBMP were reversible. Interestingly, we found that the losses in enzymatic activity, the P450 reduced CO spectrum, and the native P450 heme could be restored by approximately 20−30% following extensive dialysis of the tBA- or tBMP-inactivated samples (Table 2 and data not shown). Similar results were obtained with P450 2B4 isolated from rabbit liver (data not shown). In comparison to the tBA-inactivated P450 2E1 T303A samples that restored their losses in activity and the reduced CO spectrum to 100% (*32*), the acetylene-inactivated 2B4 and 2B4 T302A samples were only partially reversible (20−30% restoration). These data indicate a possible difference in the mechanism of reversibility between P450 2E1 T303A and the 2B4 P450s.

The formation of stable heme adducts following the inactivation of P450 2E1 T303A by tBA was previously shown to be dependent upon the addition of an external source of protons to the enzyme, such as those provided by a strong acid (*33*). However, the tBA-inactivated wild-type 2E1 enzyme was able to form stable adducts in the absence of an external proton supply, suggesting a role for the T303 in the donation of protons to the active site (*33*). In contrast to what was previously observed with tBA-inactivated P450 2E1, preacidification of both the tBA-inactivated wild-type 2B4 and 2B4 T302A samples was required in order to observe the two tBA adducts under nonacidic LC-MS/MS conditions (Table 3). Similarly, the tBMP-inactivated P450 2B4 T302A mutant required the addition of acid to generate stable heme adducts. Therefore, a source of protons or preacidification is required in both the wild-type and T302A mutant samples in order to detect stable acetylene heme adducts. These data suggest that, unlike the T303 residue in P450 2E1, the T302 residue in P450 2B4 is not involved in the delivery of protons required to form the tBA or tBMP heme products. Although a lack of acetylene heme adduct formation in the absence of protons indicates that proton delivery to the tBA− or tBMP−heme complex is inefficient in the 2B4 P450s, it does not preclude the T302 residue from participating in the positioning of crucial waters in the enzyme active site or from donating protons to the activated oxygen species during enzyme catalysis.

We have recently reported that a bridged intermediate between the heme iron, the oxygen-inserted tBA, and one pyrrole nitrogen of the heme moiety was responsible for the reversible loss in the enzymatic activity of the 2E1 T303A mutant (*64*). This intermediate could be detected spectrally at 485 nm and had two possible fates: (1) the formation of the intermediate was reversible, or (2) in the presence of exogenously supplied protons (similar to the native proton transfer pathway involving T303 in the parent 2E1 enzyme) the intermediate could modify the P450 heme by *N*-alkylation. In the presence of protons, cleavage of the intermediate leads to the formation of a stable, inactive, tBA-labeled heme product. The preacidification of our samples through the addition of TFA may have allowed for the directed delivery of protons to occur via an alternate pathway within the active site of the T303A mutant; a greater access of water molecules to the T303A active site may restore proton transfer. Our MS/MS spectral data and the absence of any spectral intermediate at 485 nm in the tBA-inactivated 2B4 and 2B4 T302A samples (data not shown) support our conclusions that a role for T302 in the mechanism of reversibility and in the delivery of protons to the acetylene−iron complex is absent in P450 2B4.

Crystal structure determinations of several bacterial P450s show that the highly conserved threonine residue is located in the I helix near the proposed oxygen binding pocket and that it is within hydrogen-bonding distance to the peroxo-iron oxidant species (*9*−*11*). In support of the proposed role of this residue in a proton delivery network, the rates of camphor hydroxylation by $P450_{cam}$ (*26*, *27*) and fatty acid hydroxylation by BM-3 (*65*) were significantly diminished when this residue was mutated to an alanine. Makris and Sligar proposed that in the absence of the threonine hydroxyl group at position 252 in $P450_{cam}$, the second proton could not be transferred to the reduced dioxygen complex and, therefore, the oxyferryl intermediate required for hydroxylation could not be generated (*66*, *67*). Vaz et al. have demonstrated that the threonine 302 to alanine mutant of P450 2B4 primarily uses the peroxo heme complex as the oxidant species for insertion of oxygen into substrates, whereas the wild-type 2B4 utilizes the classic oxenoid-iron species (*29*). On the basis of these observations, we investigated the inactivation of P450s 2B4 and 2B4 T302A by tBA in a reductase- and NADPH-free system. Since artificial oxidants have previously been shown to support the metabolism of various substrates by P450s and the inactivation of P450s by different compounds (*54*−*56*), we tested the ability of hydrogen peroxide and cumene hydroperoxide to act as artificial oxidants in our system. Hydrogen peroxide preferentially forms the peroxo-iron oxidant species whereas the oxenoid-iron species is generated by cumene hydroperoxide. We found that cumene hydroperoxide could support the activities of P450s 2B4 and 2B4 T302A as well as their inactivation by tBA (Table 4). The inactivation of P450 2B4 and the T302A mutant of 2B4 by tBA in the cumene hydroperoxide-supported system was shown to occur primarily through the formation of tBA adducts to the P450 hemes. Although hydrogen peroxide supported the 7-EFC *O*-deethylation activity of the 2B4 P450s, inactivation of these enzymes by tBA was not observed. These data suggest that the oxenoid-iron species is the primary oxidant involved in the inactivation of the 2B4 P450s by tBA in the alternate oxidant-supported system and that, unlike what is observed with P450 2E1 T303A in the same system, there does not appear to be a disruption in proton delivery to the active site of the T302A mutant of 2B4. While Vaz and Coon reported the use of a peroxo heme species for the oxygenation of substrate and a role for T302 in proton delivery (*29*), our data in the surrogate oxidant system suggest that the 2B4 T302A enzyme does not utilize the peroxo heme complex during inactivation by tBA. Since the wild-type and mutant 2B4 enzymes appear to utilize the oxenoid-iron species during inactivation by tBA, it appears that the conserved

T302 residue may not contribute to the delivery of protons to the activated oxygen species in the artificial oxidant system. Although surrogate oxidants may not directly compare to a system containing reductase and NADPH, these data are consistent with our MS/MS spectral data and computational data which suggest a lack of involvement of the conserved T302 in tBA-dependent inactivation, proton delivery to the acetylene−heme complex, and reversibility.

Computational studies of tBA and tBMP inactivation based on models of P450s 2B4 and 2B4 T302A indicate numerous low-energy bound inhibitor configurations proximate to the active oxygen species. The energy-based docked configurations observed were, in fact, effective reactant configurations for oxygen insertion, as evident from quantum chemical investigations in progress (Harris, Blobaum, and Hollenberg, in preparation), which suggest close approaches of the unsaturated bond are required for initiation of the rate-determining oxygen insertion step following the formation of the oxenoid-iron species. The docked configurations were found to be dynamically stable. In short, exploratory molecular dynamics simulations indicated temporally preferred orientations commensurate with the initial docking results. The greater access over the A and D pyrrole rings in the 2B4 model is consistent with the results suggested by experiment that *N*-alkyl adduction takes place via these heme ring components.

Glutamate 301 (E301) in 2B4 was found to have significant "residence" times in the substrate/inhibitor/heme binding site with some plasticity in orientation. As a consequence of this glutamate disposition, the hydrogen bond networks in both the wild-type 2B4 and T302A enzymes would allow facile proton transfer directly from the E301, via intervening binding site waters to the heme-bound peroxo species without an intervening T302. MD equilibration of models of 2B4 T302A starting from initial coordinates without a contiguous network between E301 and the heme-bound peroxo led to configurations in which structural waters "moved in" to effectively substitute for the missing T302 linkage. Both the exposure of the E301 in the substrate/inhibitor binding site and the size of the cavity lead to compensatory proton transfer networks being established despite the T302A mutation in the case of the tBA-bound system. Studies in progress indicate that the stability of such compensatory networks involving positioning of new waters to form proton networks may be substrate dependent. The present results, however, are consistent with the minimal modulation in binding, inactivation, and stabilization of the suicide substrate interactions with tBA and tBMP due to the T302A mutation and suggest a plausible rationale for the very minor perturbation in 2B4.

It is evident from the results presented here that the relative size and architecture of the enzyme active site play an influential role in the inactivation of P450s 2E and 2B by small acetylenes and that these differences contribute to the reversibility of inactivation. Likewise, our results also indicate that distinct differences in inactivator structure influence the type of adduct that is formed as well as the accessibility of the heme pyrrole rings for adduct formation in acetylene-mediated P450 inactivation events. Continued refinement and computational studies based on models of the wild-type and mutant P450s 2E1 and 2B4, along with work based on the new crystal structures of 2B4 with acetylene inactivators docked in the active sites, will aid in the interpretation of our results and will facilitate our understanding of the differences observed between P450s 2E1 and 2B4 and between the mechanism-based inactivations of these proteins by tBA and tBMP.

ACKNOWLEDGMENT

We thank Dr. Ute Kent at the University of Michigan and Dr. William Alworth at Tulane University for informative discussions. D.L.H. acknowledges an award of supercomputer support at the Pittsburgh Supercomputer Center through Grant MCP9900032P.

REFERENCES

1. Gonzalez, F. J. (1988) The molecular biology of cytochrome P450s, *Pharmacol. Rev. 40*, 243−288.
2. Nelson, D. R., Koymans, L., Kamataki, T., Stegeman, J. J., Feyereisen, R., Waxman, D. J., Waterman, M. R., Gotoh, O., Coon, M. J., Estabrook, R. W., Gunsalus, I. C., and Nebert, D. W. (1996) P450 superfamily: update on new sequences, gene mapping, accession numbers and nomenclature, *Pharmacogenetics 6*, 1−42.
3. Porter, T. D., and Coon, M. J. (1991) Cytochrome P-450. Multiplicity of isoforms, substrates, and catalytic and regulatory mechanisms, *J. Biol. Chem. 266*, 13469−13472.
4. White, R. E., and Coon, M. J. (1980) Oxygen activation by cytochrome P-450, *Annu. Rev. Biochem. 49*, 315−356.
5. Guengerich, F. P., and Shimada, T. (1991) Oxidation of toxic and carcinogenic chemicals by human cytochrome P-450 enzymes, *Chem. Res. Toxicol. 4*, 391−407.
6. Kent, U. M., Juschyshyn, M. I., and Hollenberg, P. F. (2001) Mechanism-based inactivators as probes of cytochrome P450 structure and function, *Curr. Drug Metab. 2*, 215−243.
7. Halpert, J. R. (1995) Structural basis of selective cytochrome P450 inhibition, *Annu. Rev. Pharmacol. Toxicol. 35*, 29−53.
8. Johnson, E. F., Kronbach, T., and Hsu, M. H. (1992) Analysis of the catalytic specificity of cytochrome P450 enzymes through site-directed mutagenesis, *FASEB J. 6*, 700−705.
9. Poulos, T. L., Finzel, B. C., and Howard, A. J. (1987) High-resolution crystal structure of cytochrome P450cam, *J. Mol. Biol. 195*, 687−700.
10. Ravichandran, K. G., Boddupalli, S. S., Hasermann, C. A., Peterson, J. A., and Deisenhofer, J. (1993) Crystal structure of hemoprotein domain of P450BM-3, a prototype for microsomal P450's, *Science 261*, 731−736.
11. Hasemann, C. A., Ravichandran, K. G., Peterson, J. A., and Deisenhofer, J. (1994) Crystal structure and refinement of cytochrome P450terp at 2.3 Å resolution, *J. Mol. Biol. 236*, 1169−1185.
12. Scott, E. E., He, Y. A., Wester, M. R., White, M. A., Chin, C. C., Halpert, J. R., Johnson, E. F., and Stout, C. D. (2003) An open conformation of mammalian cytochrome P450 2B4 at 1.6-Å resolution, *Proc. Natl. Acad. Sci. U.S.A. 100*, 13196−13201.
13. Scott, E. E., White, M. A., He, Y. A., Johnson, E. F., Stout, C. D., and Halpert, J. R. (2004) Structure of mammalian cytochrome P450 2B4 complexed with 4-(4-chlorophenyl)imidazole at 1.9-Å resolution: insight into the range of P450 conformations and the coordination of redox partner binding, *J. Biol. Chem. 279*, 27294−27301.
14. Wester, M. R., Yano, J. K., Schoch, G. A., Yang, C., Griffin, K. J., Stout, C. D., and Johnson, E. F. (2004) The structure of human microsomal cytochrome P450 2C9 complexed with flurbiprofen at 2.0 Å resolution, *J. Biol. Chem*. (in press).
15. Wester, M. R., Johnson, E. F., Marques-Soares, C., Dijols, S., Dansette, P. M., Mansuy, D., and Stout, C. D. (2003) Structure of mammalian cytochrome P450 2C5 complexed with diclofenac at 2.1 Å resolution: evidence for an induced fit model of substrate binding, *Biochemistry 42*, 9335−9345.
16. Roberts, E. S., Hopkins, N. E., Alworth, W. L., and Hollenberg, P. F. (1993) Mechanism-based inactivation of cytochrome P450 2B1 by 2-ethynylnaphthalene: identification of an active-site peptide, *Chem. Res. Toxicol. 6*, 470−479.

17. Roberts, E. S., Hopkins, N. E., Zaluzec, E. J., Gage, D. A., Alworth, W. L., and Hollenberg, P. F. (1994) Identification of active-site peptides from ^{3}H-labeled 2-ethynylnaphthalene-inactivated P450 2B1 and 2B4 using amino acid sequencing and mass spectrometry, *Biochemistry 33*, 3766−3771.
18. Roberts, E. S., Ballou, D. P., Hopkins, N. E., Alworth, W. L., and Hollenberg, P. F. (1995) Mechanistic studies of 9-ethynylphenanthrene-inactivated cytochrome P450 2B1, *Arch. Biochem. Biophys. 323*, 303−312.
19. Roberts, E. S., Hopkins, N. E., Zaluzec, E. J., Gage, D. A., Alworth, W. L., and Hollenberg, P. F. (1995) Mechanism-based inactivation of cytochrome P450 2B1 by 9-ethynylphenanthrene, *Arch. Biochem. Biophys. 323*, 295−302.
20. Roberts, E. S., Pernecky, S. J., Alworth, W. L., and Hollenberg, P. F. (1996) A role for threonine 302 in the mechanism-based inactivation of P450 2B4 by 2-ethynylnaphthalene, *Arch. Biochem. Biophys. 331*, 170−176.
21. Ortiz de Montellano, P. R. (1985) Alkenes and alkynes, in *Bioactivation of Foreign Compounds* (Anders, M. W., Ed.) pp 121−155, Academic Press, New York.
22. Ortiz de Montellano, P. R., and Reich, N. O. (1986) Inhibition of cytochrome P450 enzymes, in *Cytochrome P450: Structure, Mechanism, and Biochemistry* (Ortiz de Montellano, P. R., Ed.) pp 273−314, Plenum Press, New York.
23. Ortiz de Montellano, P. R., and Komives, E. A. (1985) Branchpoint for heme alkylation and metabolite formation in the oxidation of arylacetylenes by cytochrome P-450, *J. Biol. Chem. 260*, 3330−3336.
24. Komives, E. A., and Ortiz de Montellano, P. R. (1987) Mechanism of oxidation of pi bonds by cytochrome P-450. Electronic requirements of the transition state in the turnover of phenylacetylenes, *J. Biol. Chem. 262*, 9793−9802.
25. Kunze, K. L., Mangold, B. L., Wheeler, C., Beilan, H. S., and Ortiz de Montellano, P. R. (1983) The cytochrome P-450 active site. Regiospecificity of prosthetic heme alkylation by olefins and acetylenes, *J. Biol. Chem. 258*, 4202−4207.
26. Imai, M., Shimada, H., Watanabe, Y., Matsushima-Hibiya, Y., Makino, R., Koga, H., Horiuchi, T., and Ishimura, Y. (1989) Uncoupling of the cytochrome P-450cam monooxygenase reaction by a single mutation, threonine-252 to alanine or valine: possible role of the hydroxy amino acid in oxygen activation, *Proc. Natl. Acad. Sci. U.S.A. 86*, 7823−7827.
27. Martinis, S. A., Atkins, W. M., Stayton, P. S., and Sligar, S. G. (1989) A conserved residue of cytochrome P-450 is involved in heme-oxygen stability and activation, *J. Am. Chem. Soc. 111*, 9252−9253.
28. Raag, R., Martinis, S. A., Sligar, S. G., and Poulos, T. L. (1991) Crystal structure of the cytochrome P-450CAM active site mutant Thr252Ala, *Biochemistry 30*, 11420−11429.
29. Vaz, A. D., Pernecky, S. J., Raner, G. M., and Coon, M. J. (1996) Peroxo-iron and oxenoid-iron species as alternative oxygenating agents in cytochrome P450-catalyzed reactions: switching by threonine-302 to alanine mutagenesis of cytochrome P450 2B4, *Proc. Natl. Acad. Sci. U.S.A. 93*, 4644−4648.
30. Vaz, A. D., McGinnity, D. F., and Coon, M. J. (1998) Epoxidation of olefins by cytochrome P450: evidence from site-specific mutagenesis for hydroperoxo-iron as an electrophilic oxidant, *Proc. Natl. Acad. Sci. U.S.A. 95*, 3555−3560.
31. Vaz, A. D. (2001) Multiple oxidants in cytochrome P450 catalyzed reactions: implications for drug metabolism, *Curr. Drug Metab. 2*, 1−16.
32. Blobaum, A. L., Kent, U. M., Alworth, W. L., and Hollenberg, P. F. (2002) Mechanism-based inactivation of cytochromes P450 2E1 and 2E1 T303A by *tert*-butyl acetylenes: characterization of reactive intermediate adducts to the heme and apoprotein, *Chem. Res. Toxicol. 15*, 1561−1571.
33. Blobaum, A. L., Kent, U. M., Alworth, W. L., and Hollenberg, P. F. (2004) Novel reversible inactivation of cytochrome P450 2E1 T303A by *tert*-butyl acetylene: The role of threonine 303 in proton delivery to the active site of cytochrome P450 2E1, *J. Pharmacol. Exp. Ther. 310*, 281−290.
34. von Weymarn, L. B., Blobaum, A. L., and Hollenberg, P. F. (2004) The mechanism-based inactivation of p450 2B4 by *tert*-butyl 1-methyl-2-propynyl ether: structural determination of the adducts to the p450 heme, *Arch. Biochem. Biophys. 425*, 95−105.
35. Bridges, A., Gruenke, L., Chang, Y. T., Vakser, I. A., Loew, G., and Waskell, L. (1998) Identification of the binding site on cytochrome P450 2B4 for cytochrome b5 and cytochrome P450 reductase, *J. Biol. Chem. 273*, 17036−17049.
36. Hanna, I. H., Teiber, J. F., Kokones, K. L., and Hollenberg, P. F. (1998) Role of the alanine at position 363 of cytochrome P450 2B2 in influencing the NADPH- and hydroperoxide-supported activities, *Arch. Biochem. Biophys. 350*, 324−332.
37. Buters, J. T., Schiller, C. D., and Chou, R. C. (1993) A highly sensitive tool for the assay of cytochrome P450 enzyme activity in rat, dog and man. Direct fluorescence monitoring of the deethylation of 7-ethoxy-4-trifluoromethylcoumarin, *Biochem. Pharmacol. 46*, 1577−1584.
38. Omura, T., and Sato, R. (1964) The carbon monoxide-binding pigment of liver microsomes, *J. Biol. Chem. 239*, 2370−2378.
39. Harris, D. L., Park, J. Y., Gruenke, L., and Waskell, L. (2004) Theoretical study of the ligand-CYP2B4 complexes: effect of structure on binding free energies and heme spin state, *Proteins 55*, 895−914.
40. Cornell, W. D., Cieplak, P., Bayly, C. I., Gould, I. R., Merz, K. M., Ferguson, D. M., Spellmeyer, D. C., Fox, T., Caldwell, J. W., and Kollman, P. A. (1995) A second generation force field for the simulation of proteins, nucleic acids, and organic molecules, *J. Am. Chem. Soc. 117*, 5179−5197.
41. Park, J. Y., and Harris, D. (2003) Construction and assessment of models of CYP2E1: predictions of metabolism from docking, molecular dynamics, and density functional theoretical calculations, *J. Med. Chem. 46*, 1645−1660.
42. Sippl, M. J. (1993) Recognition of errors in three-dimensional structures of proteins, *Proteins 17*, 355−362.
43. Harris, D. L. (2004) In silico predictive metabolism: a structural/electronic filter method, *Curr. Opin. Drug Discov. Dev. 7*, 43−48.
44. Sali, A., and Blundell, T. L. (1993) Comparative protein modelling by satisfaction of spatial restraints, *J. Mol. Biol. 234*, 779−815.
45. Canutescu, A. A., Shelenkov, A. A., and Dunbrack, R. L., Jr. (2003) A graph-theory algorithm for rapid protein side-chain prediction, *Protein Sci. 12*, 2001−2014.
46. Mendes, J., Nagarajaram, H. A., Soares, C. M., Blundell, T. L., and Carrondo, M. A. (2001) Incorporating knowledge-based biases into an energy-based side-chain modeling method: application to comparative modeling of protein structure, *Biopolymers 59*, 72−86.
47. Zhao, D., Gilfoyle, D. J., Smith, A. T., and Loew, G. H. (1996) Refinement of 3D models of horseradish peroxidase isoenzyme C: predictions of 2D NMR assignments and substrate binding sites, *Proteins 26*, 204−216.
48. Laskowski, R. A., MacArthur, M. W., Moss, D. S., and Thornton, J. M. (1993) PROCHECK: A program to check the stereochemical quality of protein structures, *J. Appl. Crystallogr. 26*, 283−291.
49. Bayly, C., Cieplak, P., Cornell, W., and Kollman, P. (1993) A well-behaved electrostatic potential based method using charge restraints for deriving atomic charges—the RESP model, *J. Phys. Chem. 97*, 10269−10280.
50. Pearlman, D. A., Case, D. A., Caldwell, J. W., Ross, W. S., Cheatham, T. E. I., DeBolt, S., and Ferguson, D. (1995) AMBER, a package of computer programs for applying molecular mechanics, normal mode analysis, molecular dynamics and free energy calculations to simulate the structural and energetic properties of molecules, *Comput. Phys. Commun. 2*, 287−303.
51. Morris, G. M., Goodsell, D. S., Halliday, R. S., Huey, R., Hart, W. E., Belew, R. K., and Olson, A. J. (1998) Automated docking using a Lamarckian genetic algorithm and an empirical binding free energy function, *J. Comput. Chem. 19*, 1639−1662.
52. Dexter, A. F., and Hager, L. P. (1995) Transient heme N-alkylation of chloroperoxidase by terminal alkenes and alkynes, *J. Am. Chem. Soc. 117*, 817−818.
53. Debrunner, P. G., Dexter, A. F., Schulz, C. E., Xia, Y. M., and Hager, L. P. (1996) Mossbauer and electron paramagnetic resonance studies of chloroperoxidase following mechanism-based inactivation with allylbenzene, *Proc. Natl. Acad. Sci. U.S.A. 93*, 12791−12798.
54. Roberts, E. S., Lin, H., Crowley, J. R., Vuletich, J. L., Osawa, Y., and Hollenberg, P. F. (1998) Peroxynitrite-mediated nitration of tyrosine and inactivation of the catalytic activity of cytochrome P450 2B1, *Chem. Res. Toxicol. 11*, 1067−1074.
55. Anari, M. R., Khan, S., Liu, Z. C., and O'Brien, P. J. (1995) Cytochrome P450 peroxidase/peroxygenase mediated xenobiotic metabolic activation and cytotoxicity in isolated hepatocytes, *Chem. Res. Toxicol. 8*, 997−1004.

56. Yanev, S. G., Kent, U. M., Roberts, E. S., Ballou, D. P., and Hollenberg, P. F. (2000) Mechanistic studies of cytochrome P450 2B1 inactivation by xanthates, *Arch. Biochem. Biophys. 378*, 157−166.
57. Wester, M. R., Johnson, E. F., Marques-Soares, C., Dansette, P. M., Mansuy, D., and Stout, C. D. (2003) Structure of a substrate complex of mammalian cytochrome P450 2C5 at 2.3 Å resolution: evidence for multiple substrate binding modes, *Biochemistry 42*, 6370−6379.
58. Wallner, B., and Elofsson, A. (2003) Can correct protein models be identified?, *Protein Sci. 12*, 1073−1086.
59. Harris, D. L. (2002) Oxidation and electronic state dependence of proton transfer in the enzymatic cycle of cytochrome P450eryF, *J. Inorg. Biochem. 91*, 568−585.
60. Guallar, V., Harris, D. L., Batista, V. S., and Miller, W. H. (2002) Proton-transfer dynamics in the activation of cytochrome P450eryF, *J. Am. Chem. Soc. 124*, 1430−1437.
61. Harris, D. L., and Hudson, B. S. (1991) Fluorescence and molecular dynamics study of the internal motion of the buried tryptophan in bacteriophage T4 lysozyme: Effects of temperature and alteration of nonbonded networks, *Chem. Phys. 158*, 353−382.
62. Xu, J., Baase, W. A., Quillin, M. L., Baldwin, E., and Matthews, B. W. (2001) Structural and thermodynamic analysis of the binding of solvent at internal sites in T4 lysozyme, *Protein Sci. 10*, 1067−1078.
63. Mackman, R., Guo, Z., Guengerich, F. P., and Ortiz de Montellano, P. R. (1996) Active site topology of human cytochrome P450 2E1, *Chem. Res. Toxicol. 9*, 223−226.
64. Blobaum, A. L., Lu, Y., Kent, U. M., Wang, S., and Hollenberg, P. F. (2004) Formation of a novel reversible cytochrome P450 spectral intermediate: role of threonine 303 in P450 2E1 inactivation, *Biochemistry 43*, 11942−11952.
65. Yeom, H., Sligar, S. G., Li, H., Poulos, T. L., and Fulco, A. J. (1995) The role of Thr268 in oxygen activation of cytochrome P450BM-3, *Biochemistry 34*, 14733−14740.
66. Makris, T. M., Davydov, R., Denisov, I. G., Hoffman, B. M., and Sligar, S. G. (2002) Mechanistic enzymology of oxygen activation by the cytochromes P450, *Drug Metab. Rev. 34*, 691−708.
67. Jin, S., Makris, T. M., Bryson, T. A., Sligar, S. G., and Dawson, J. H. (2003) Epoxidation of olefins by hydroperoxo-ferric cytochrome P450, *J. Am. Chem. Soc. 125*, 3406−3407.

BI0478953